Hindawi Publishing Corporation
International Journal of Photoenergy
Volume 2012, Article ID 135132, 8 pages
doi:10.1155/2012/135132

Research Article

Photocatalytic Properties of Nitrogen-Doped $Bi_{12}TiO_{20}$ Synthesized by Urea Addition Sol-Gel Method

Jiyong Wei, Baibiao Huang, Peng Wang, Zeyan Wang, Xiaoyan Qin, Xiaoyang Zhang, Xiangyang Jing, Haixia Liu, and Jiaoxian Yu

State Key Laboratory of Crystal Materials, Institute of Crystal Materials, Shandong University, Jinan 250100, China

Correspondence should be addressed to Baibiao Huang, bbhuang@sdu.edu.cn

Received 25 July 2011; Revised 19 September 2011; Accepted 30 September 2011

Academic Editor: Jiaguo Yu

Undoped and nitrogen-doped $Bi_{12}TiO_{20}$ materials were synthesized by urea addition sol-gel method. By adding urea, undoped, and N-doped gel-type precursors were synthesized by low-temperature dehydrolyzation. Nitrogen-doped and undoped nanocrystalline $Bi_{12}TiO_{20}$ were prepared by annealing at 600∘C for 30 minutes. From UV-Vis absorption and diffuse reflection spectrum, the absorbing band shifted from 420 to 500 nm by nitrogen doping. The bonds of Ti–N and N–O were identified by XPS spectra from the prepared materials, and the enhancement of visible light absorption was attributed to nitrogen's substitution of oxygen. Photocatalytic properties of prepared materials were characterized by the decomposition of Rhodamine B illuminated by whole spectra of 300 W Xe light. The photocatalyst $Bi_{12}TiO_{20-y}N_y$ ($y = 0.03$) with N/(N+O) mole ratio about 3% shows better performance than that of heavily doped $Bi_{12}TiO_{20-z}N_z$ ($z = 0.06$), undoped $Bi_{12}TiO_{20}$, and light-doped $Bi_{12}TiO_{20-x}N_x$ ($x = 0.01$) photocatalysts due to its better crystalline morphology.

1. Introduction

Environmental and energetic problems are great challenges for human beings now. The photosensitized electrolytic oxidation [1] and the electrochemical photolysis of water [2] on TiO_2 electrode performed by Fujishima and Honda offered some solutions. In recent years, TiO_2 and other photocatalysts have been extensively studied for environmental pollutant treatment [3] such as water disinfection [4].

However, wide bandgap semiconductor photocatalysts, such as TiO_2, can only absorb UV light, which only take 4% of the whole solar spectra owing to the wide bandgap. In order to expand the absorption spectra region of TiO_2, doping with nonmetallic atoms, such as nitrogen, fluorine and sulfur has been developed [5–18]. The conventional doping processes reported were commonly by the annealing of prepared TiO_2 materials in NH_3 or other dopant atmospheres [5–8]. Rengifo-Herrera et al. have reported N, S codoped commercial TiO_2 powders [17] which were doped by the decomposition of thiourea as a nitrogen and sulfur source. Effects of calcination temperatures [19], morphologies [20], and composite [21] on photocatalytic activity were also studied.

Recently, photocatalysts containing ion units of $(Bi_2O_2)^{2+}$, such as Bi_2WO_6 [22, 23] and bismuth titanate were extensively studied for the photocatalytic splitting of water and the photodegradation of organic pollutants. Bismuth titanate was a wide bandgap semiconductor with several crystal phases: ferroelectric perovskite phase ($Bi_4Ti_3O_{12}$), dielectric pyrochlorite phase ($Bi_2Ti_2O_7$), refractive sillenite phase ($Bi_{12}TiO_{20}$), and so forth. Kudo and Hijii have studied bismuth titanate as potential photocatalyst [22]. Yao et al. [24–27] and other groups [28–36] explored nano crystalline materials of $Bi_{12}TiO_{20}$ as visible light photocatalysts, and the as-prepared materials showed high photocatalytic activity for decomposing organic dyes under ultraviolet light irradiation. The further expansion of $Bi_{12}TiO_{20}$ material's absorption to visible region is very important for the visible light responsive photocatalytic activity, because $Bi_{12}TiO_{20}$ can only absorb light with wavelength below 420 nm (about 2.9 eV) [21–24]. Little work has been performed for nonmetallic (such as nitrogen and carbon) doping of bismuth titanate crystals, though the doping of $Bi_{12}TiO_{20}$ nano- or single crystals with metal element [25, 26] and nonmetallic element such as P for the influence of refractive optical properties has been studied [37].

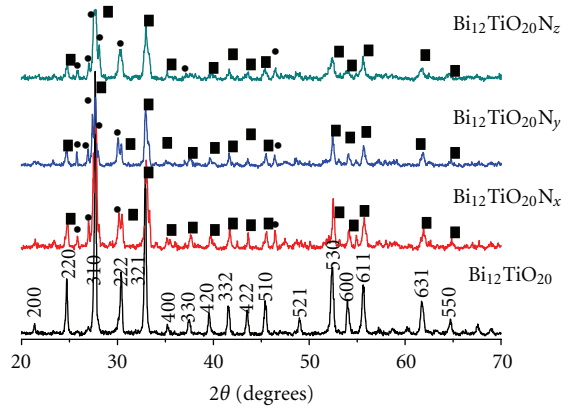

Figure 1: XRD spectrum of bismuth titanate: $Bi_{12}TiO_{20}$, $Bi_{12}TiO_{20-x}N_x$ ($x = 0.01$), $Bi_{12}TiO_{20-y}N_y$ ($y = 0.03$), and $Bi_{12}TiO_{20-z}N_z$ ($z = 0.06$).

In this paper, nitrogen-doped bismuth titanate powders and films were prepared by sol-gel method and dip-coating method, respectively, the nitrogen dopant was introduced by the adding of urea in precursor solutions as additives, which is widely used as fertilizer. Urea can be dissolved in water and other polar solvents, and can release free $NH_2^\bullet$ radicals as nitrogen sources during thermal decomposition. After preparation of urea included sol-gel precursors, high-temperature annealing was applied to undoped and doped $Bi_{12}TiO_{20}$ precursors for crystallization and also for the in-place nitrogen doping by urea decomposing. The results of whole-spectra photocatalytic activities of nitrogen-doped and undoped $Bi_{12}TiO_{20}$ were presented by the photodegradation of rhodamine b (RB) solutions.

2. Experimental Details

Undoped and nitrogen-doped $Bi_{12}TiO_{20}$ nanocrystalline powders and films were prepared by sol-gel method and dip coating. Chemical agents of analytical grade were used in the experiments, such as acetic acid, $Bi(NO_3)_3 \cdot 5H2O$ and $Ti(OC_4H_9)_4$. Reagents were dissolved in ethylene glycol monomethyl ether solution while urea was used as nitrogen additive. Crystalline materials of undoped and nitrogen-doped $Bi_{12}TiO_{20}$ were prepared by annealing of the sol-gel precursors at temperature of 600°C for about 30 minutes.

2.1. Preparation of $Bi_{12}TiO_{20}$ and Nitrogen-Doped $Bi_{12}TiO_{20}$ Crystalline Materials. The mole ratio of reagents $Bi(NO_3)_3 \cdot 5H_2O$ and $Ti(OC_4H_9)_4$ was 12 : 1 in the precursor solution for preparation of $Bi_{12}TiO_{20}$ and $Bi_{12}TiO_{20-x}N_x$ ($x = 0.01$), $Bi_{12}TiO_{20-y}N_y$ ($y = 0.03$), and $Bi_{12}TiO_{20-z}N_z$ ($z = 0.06$) sol-gel precursors, with additional urea added for nitrogen-doped materials (molecule ratio of $NH_2^\bullet : Bi^{3+}$ about 0 : 1, 1 : 1, 2 : 1, and 3 : 1 in sol-gel). The reagents were blended in acetic acid and ethylene glycol monomethyl ether solutions, and were dried by infrared light to get the gel. $Bi_{12}TiO_{20}$ and $Bi_{12}TiO_{20-x}N_x$ ($x = 0.01$), $Bi_{12}TiO_{20-y}N_y$ ($y = 0.03$), and $Bi_{12}TiO_{20-z}N_z$ ($z = 0.06$) sillenite phase crystalline powders were obtained by annealing the gel precursors at 600°C for about 30 minutes.

2.2. Preparation of $Bi_{12}TiO_{20}$ Crystalline Films for UV-Vis Absorption Characterization. Crystalline films of $Bi_{12}TiO_{20}$, $Bi_{12}TiO_{20-x}N_x$ ($x = 0.01$), $Bi_{12}TiO_{20-y}N_y$ ($y = 0.03$), and $BBi_{12}TiO_{20-z}N_z$ ($z = 0.06$) were prepared by dipping glass chips into the prepared sol-gel precursor solutions, and then were dried by infrared light, and annealed at 600°C for 30 minutes in nitrogen atmosphere.

2.3. Characterization Methods. The crystal phases of prepared powders were identified by X-ray diffraction (XRD, Cu K_α, D/max-ra X-ray). Morphology of the doped and undoped $Bi_{12}TiO_{20}$ nanocrystals was characterized by scanning electron microscopy (SEM, JEOL JSM6700F). The compositions and the electron bonding states of nitrogen-doped $Bi_{12}TiO_{20}$ were characterized by X-ray photoelectron spectroscopy (XPS, ESCALAB 250 of Thermal Fisher Scientific). To study the red shift of absorption wavelength of nitrogen-doped materials, UV-Vis absorption spectra of $Bi_{12}TiO_{20}$ crystalline films were performed by UV-Vis spectrophotometer (U-3500, 187 nm–3500 nm). The UV-Vis diffuse reflection spectra of doped and undoped $Bi_{12}TiO_{20}$ powders were characterized by UV/Vis spectroscopy (UV-2550, Shimadzu). Photocatalytic activity of undoped and nitrogen-doped $Bi_{12}TiO_{20}$ was characterized by the photodegradation of rhodamine b (RhB) solutions under the irradiation of 300 W Xe arc lamp (focused through a shutter window). The efficiency of the degradation processes was evaluated by monitoring the dye decolorization at the maximum absorption around 557 nm as a function of irradiation time in the separated RhB solution with a UV-vis spectrophotometer (UV-7502PC, Xinmao, Shanghai).

3. Results and Discussion

3.1. X-Ray Characterization. The crystal phases of synthesized doped and undoped nano crystalline materials were identified by X-ray diffraction. The XRD spectra of annealed $Bi_{12}TiO_{20}$, $Bi_{12}TiO_{20-x}N_x$ ($x = 0.01$), $Bi_{12}TiO_{20-y}N_y$ ($y = 0.03$), and $Bi_{12}TiO_{20-z}N_z$ ($z = 0.06$) were shown in Figure 1. No phase transformation of $Bi_{12}TiO_{20}$ structure (JCPDS no.78–1158) was observed by adding of urea as nitrogen

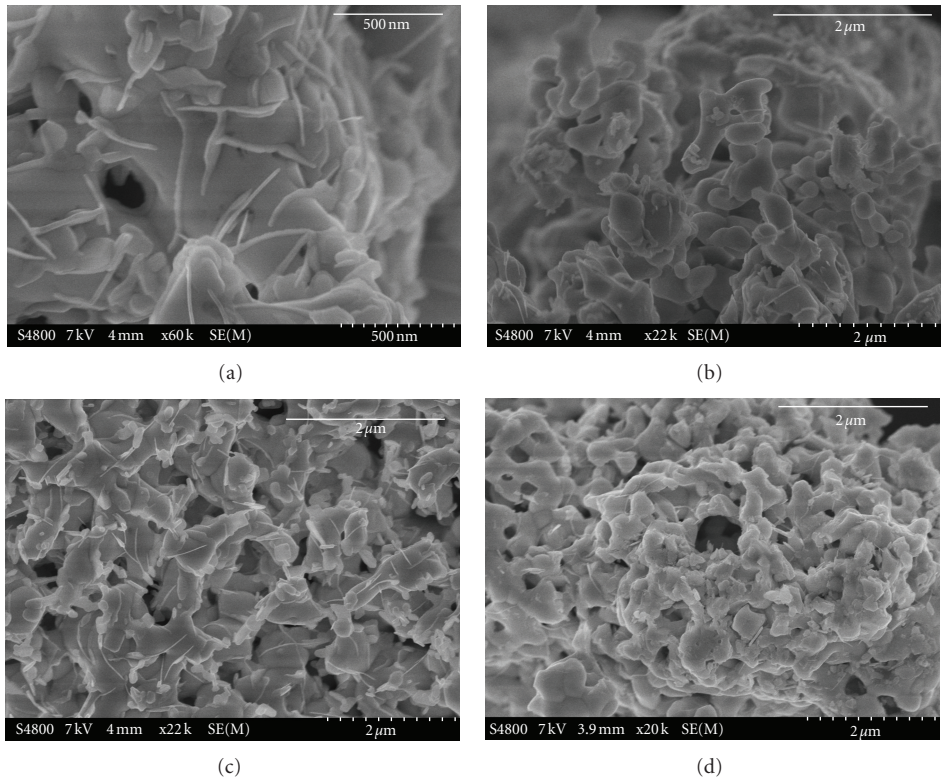

FIGURE 2: Morphologies of annealed undoped and nitrogen-doped $Bi_{12}TiO_{20}$ micro- and nano crystals observed by SEM: (a) $Bi_{12}TiO_{20}$; (b) $Bi_{12}TiO_{20-x}N_x$ ($x = 0.01$); (c) $Bi_{12}TiO_{20-y}N_y$ ($y = 0.03$); (d) $Bi_{12}TiO_{20-z}N_z$ ($z = 0.06$).

additive. The slight shift and broadening of XRD peaks showed the effect of nitrogen doping in $Bi_{12}TiO_{20}$ structure materials. From Figure 1, the sharp diffraction peak and strong intensity of $Bi_{12}TiO_{20}$ indicates good crystallinity; while after nitrogen doping, the diffraction peak intensity became weaker and the peaks broadened slightly. The (310) and (222) peak split into two peaks and shifted to lower angles with the increase of nitrogen dopant, which shows us there must be an increase for the interlamellar spacing of (310) and (222) crystal facets as nitrogen is doped in $Bi_{12}TiO_{20}$.

3.2. Morphology of Nanocrystalline Bismuth Titanate Materials. Morphologies of undoped and nitrogen-doped $Bi_{12}TiO_{20}$ materials prepared by sol-gel synthesis and annealing were characterized by SEM as show in Figure 2. The undoped $Bi_{12}TiO_{20}$ microgel like bulks dotted with nanoflakes were observed in Figure 2(a), with few holes due to the decomposition and elution of sol-gel precursor. With addition of urea in precursors, the decomposition eluted more gas and the microbulk became fractal bulks piled up as shown in Figures 2(b), 2(c), and 2(d); while with too much urea added, there are only fractal bulks and few nanoflakes, which may decrease the surface and refrain the photocatalytic performance of heavily nitrogen-doped $Bi_{12}TiO_{20-z}N_z$ ($z = 0.06$). The morphology of proper nitrogen-doped material is $Bi_{12}TiO_{20-y}N_y$ ($y = 0.03$), as shown in Figure 2(c), which is composed of separated nano bulks dotted with nanosheet-like crystals. The morphology of $Bi_{12}TiO_{20-y}N_y$ ($y = 0.03$) has more nano crystalline facets and larger surface areas than other samples, which would show better photocatalytic performance than the other samples.

3.3. Element Content and Doping of Nanocrystalline Bismuth Titanate Materials. The chemical bonding states of as-prepared materials were characterized by XPS as shown in Figure 3. As shown in Figure 3(a), the XPS peaks of Bi4f, C 1s, N 1s, and Ti 2p were detected. The split of nitrogen 1s peak and carbon 1s peak shown in Figures 3(b) and 3(c) indicate the variety of bonding states. The split of N1s peaks in Figure 3(b) was assigned to N 1s peaks of N–O bond (401.6 eV) [38] and N–Ti bond (396.4 eV) [39, 40]. The N/(N+O) molar ratio calculated from the XPS peak is about 3%. The broadening and split of C 1s peak shown in Figure 3(c) were assigned to CO/Bi_2O_3 (286.6 eV) and CO/TiO_2 (288.5 eV) physical absorb circumstances [41]. So most carbon in the sample is absorbed CO, and the visible light absorption enhancement is attributed to the doping of nitrogen.

3.4. UV-Vis Absorption Enhancement of Nitrogen-Doped Bismuth Titanate Nanocrystalline Films. The UV-Vis absorption spectra of bismuth titanate nano crystalline films with different nitrogen doping ratios were characterized in Figure 4(a). The absorption spectra of undoped bismuth titanate were broadened successfully by urea-assisted sol-gel growth of nitrogen doping as shown in the UV-Vis absorption spectra of $Bi_{12}TiO_{20}$ and $Bi_{12}TiO_{20-x}N_x$ ($x = 0.01$)

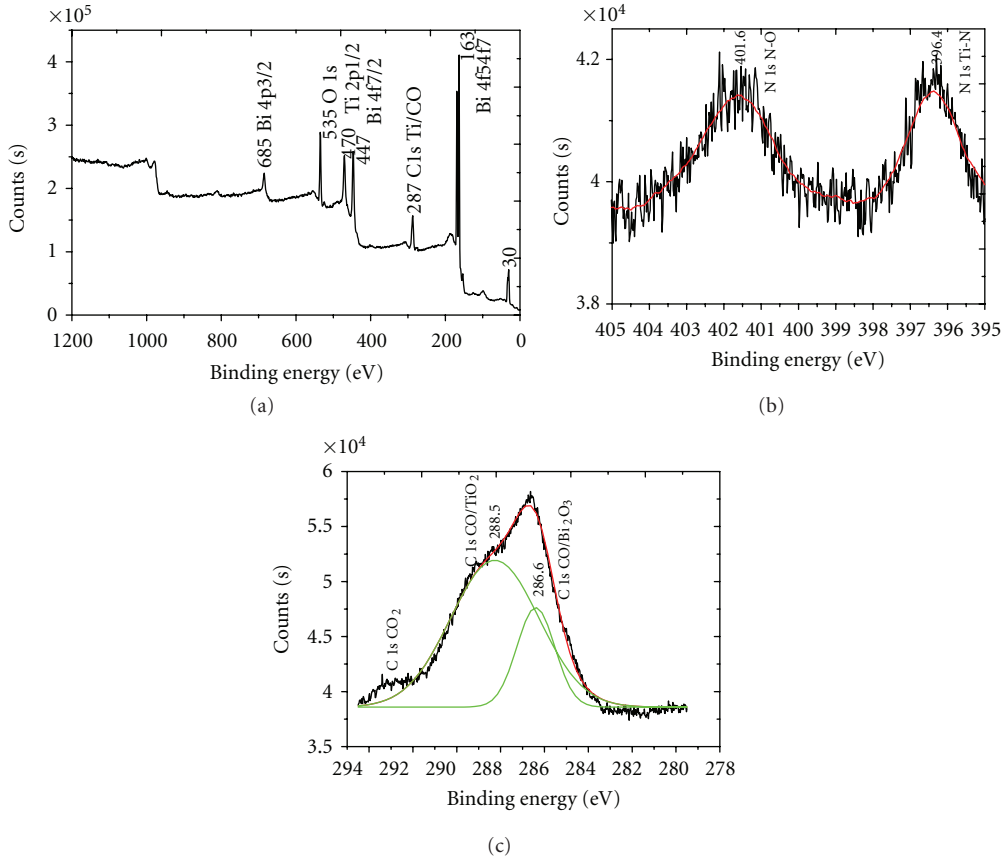

FIGURE 3: XPS absorption spectra of bismuth titanate $Bi_{12}TiO_{20-y}N_y$ ($y = 0.03$): (a) the whole spectrum of $Bi_{12}TiO_{20-y}N_y$ ($y = 0.03$); (b) spectrum of doped nitrogen; (c) spectrum of doped carbon.

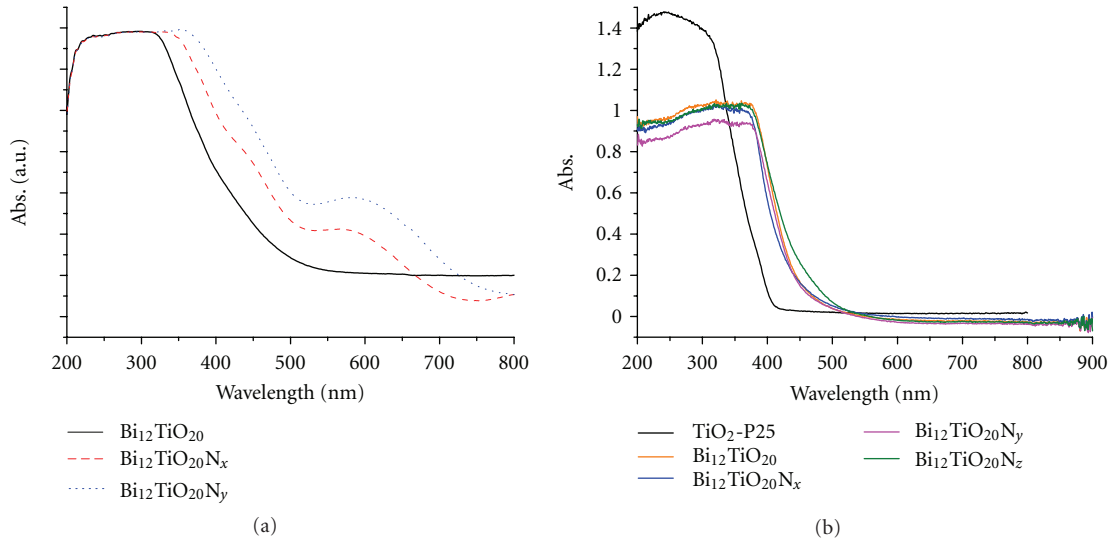

FIGURE 4: (a) Absorption spectra of films of bismuth titanate ($Bi_{12}TiO_{20}$, $Bi_{12}TiO_{20-x}N_x$ ($x = 0.01$) and $Bi_{12}TiO_{20-y}N_y$ ($y = 0.03$)) and (b) UV-Vis diffuse reflection spectra of powders $Bi_{12}TiO_{20}$, $Bi_{12}TiO_{20-x}N_x$ ($x = 0.01$), $Bi_{12}TiO_{20-y}N_y$ ($y = 0.03$), $Bi_{12}TiO_{20-z}N_z$ ($z = 0.06$), and TiO_2-P25.

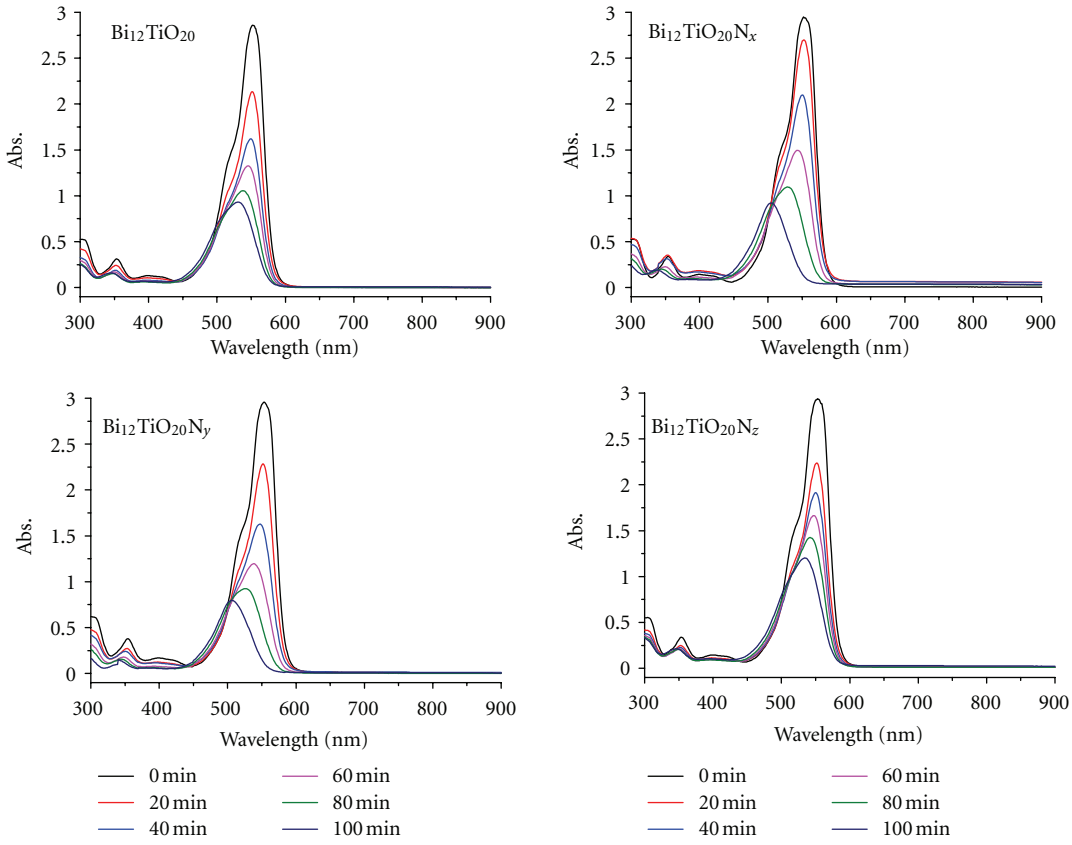

(a)

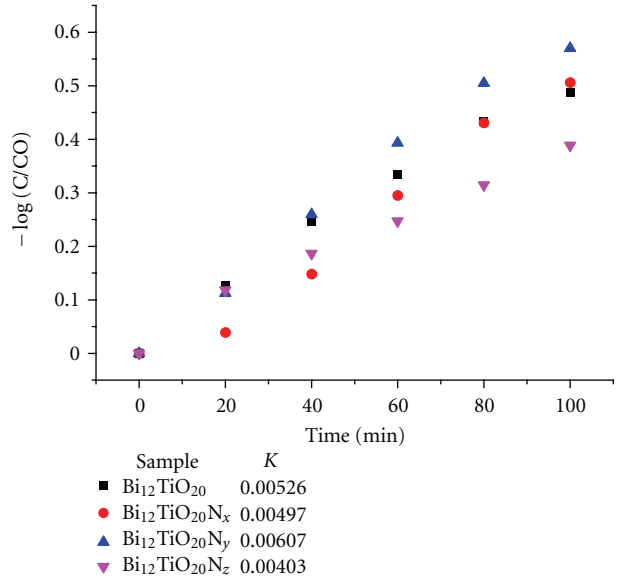

(b)

Figure 5: Photocatalytic decomposition of RhB by undoped and nitrogen-doped $Bi_{12}TiO_{20}$ photocatalysts: (a) absorption spectra decay of RhB via time; (b) decomposition activity of samples.

and $Bi_{12}TiO_{20-y}N_y$ ($y = 0.03$) films by sol-gel deposition with and without nitrogen doping. The UV-Vis absorption spectra band edge of $Bi_{12}TiO_{20}$ shifted from 400 nm to about 470 nm of nitrogen-doped $Bi_{12}TiO_{20-y}N_y$ ($y = 0.03$ with $NH_2^{\bullet}$: Bi^{3+} about 1 : 1 solution, and N/(N+O) mole ratios about 3%). The absorption spectra's broadening of nitrogen-doped $Bi_{12}TiO_{20}$ was attributed to the doping of nitrogen's substitution of oxygen site that induced the narrowing of the

bandgap. There was an additional absorption peak at 580 nm wavelength that was attributed to the deep-level nitrogen dopant.

The UV-Vis diffuse reflection spectra of nitrogen-doped and undoped $Bi_{12}TiO_{20}$ powders were characterized as shown in Figure 4(b), P25 was also used as a reference. TiO_2-P25 materials have intensive UV absorption and the absorption edge line at about 380 nm, while all $Bi_{12}TiO_{20}$ of nitrogen-doped and undoped have less UV absorption but longer bandgap-related wavelength about 450 nm. The bandgap of nitrogen-doped $Bi_{12}TiO_{20}$ *versus* undoped $Bi_{12}TiO_{20}$ in DRS spectra varied about 20 nm, from 440 nm to 460 nm. The red shift of absorption edge wavelength of nitrogen-doped $Bi_{12}TiO_{20}$ powders in DRS spectra is less than that in absorption spectra of nitrogen-doped $Bi_{12}TiO_{20}$ films, which we attribute to the variation of N/(N+O) ratios from inner to the outer layer. As known, the absorption spectra of films show the absorption of whole bulk materials, while the DRS spectrum more attribute to materials' surfaces. While annealing, there may be more nitrogen dopant in inner part and more oxygen in surfaces, so the absorption spectra edge of whole film materials will show more red shift than the diffuse reflection spectra edge obtained only from powders' surface.

The absorption band edge of $Bi_{12}TiO_{20}$ films and UV-Vis diffuse reflection band edge of $Bi_{12}TiO_{20}$ powders were successfully expanded to visible light region of solar spectra by urea-assisted sol-gel method, which would greatly enhance the utilizing ratio of visible light region of solar spectra in photocatalysis and solar cell researches.

3.5. Influence of Photocatalytic Capability of $Bi_{12}TiO_{20}$ by Nitrogen Doping. To study the relationship of photocatalytic property with nitrogen doping of bismuth titanate, photocatalysis of rhodamine b (RhB) by undoped and nitrogen-doped bismuth titanate was performed. The photocatalytic activity was characterized by the decomposition of 10 mg/L rhodamine b (RhB) solution, with 100 mg of photocatalyst added to 100 mL of rhodamine b (RhB) solution. The reaction system was irradiated by 300 W Xe lamps.

The photocatalytic ability of undoped $Bi_{12}TiO_{20}$ materials had been studied by Yao et al. [24–26] and other groups [28, 29, 31, 33, 34]. Here we are concerned with relationship of photocatalytic ability of undoped and nitrogen-doped $Bi_{12}TiO_{20}$ materials with different amount of urea added in precursors ($NH_2^{\bullet}$: Bi^{3+} about 0 : 1, 1 : 1, 2 : 1, and 3 : 1). Different amount of urea added in precursor solution deduced to the different amount of nitrogen dopant in the $Bi_{12}TiO_{20}$ photocatalysts. All samples were annealed at 600°C for 30 minutes.

As shown in Figure 5, the performance of catalyst $Bi_{12}TiO_{20}$ and $Bi_{12}TiO_{20-y}N_y$ ($y = 0.03$) have better performance than other catalysts. The undoped and nitrogen-doped $Bi_{12}TiO_{20-y}N_y$ ($y = 0.03$) catalysts with N/(N+O) mole ratio about 0% and 3% were prepared by $NH_2^{\bullet}$: Bi^{3+} about 0 : 1 and 2 : 1 in the precursor solutions, respectively.

The velocity constants of catalyst $Bi_{12}TiO_{20}$ ($k = 5.26 \times 10^{-3}\,\text{min}^{-1}$) and catalyst $Bi_{12}TiO_{20-y}N_y$ ($y = 0.03$; $k = 6.07 \times 10^{-3}\,\text{min}^{-1}$) are about 1.5-times the velocity constant of catalyst $Bi_{12}TiO_{20-z}N_z$ ($z = 0.06$; $k = 4.03 \times 10^{-3}\,\text{min}^{-1}$). So the nitrogen-doped $Bi_{12}TiO_{20-y}N_y$ ($y = 0.03$) photocatalyst with N/(N+O) mole ratio about 3% have better performance than undoped $Bi_{12}TiO_{20}$, light-doped $Bi_{12}TiO_{20-x}N_x$ ($x = 0.01$), and heavily doped $Bi_{12}TiO_{20-z}N_z$ ($z = 0.06$) photocatalysts.

The variation of whole spectra photocatalytic performance of undoped and nitrogen-doped $Bi_{12}TiO_{20}$ was attribute to the morphologies as observed by SEM in Figure 2. $Bi_{12}TiO_{20-y}N_y$ ($y = 0.03$) have more crystalline nano crystal facets and larger surface areas than other samples, which lead to better photocatalytic performance than other samples. But a high level of nitrogen-doped (above 6% of N/(N+O)) would lead to the formation of more defects in nano crystals of prepared catalysts, and would influence the transportation of photogenerated electrons and holes. Though high level of nitrogen doping can effectively expand the visible light absorption, a high defects density would lead to poor photocatalytic activity.

4. Conclusions

In conclusion, by urea-assisted sol-gel method, undoped and nitrogen-doped $Bi_{12}TiO_{20}$, $Bi_{12}TiO_{20-x}N_x$ ($x = 0.01$), $Bi_{12}TiO_{20-y}N_y$ ($y = 0.03$), and $Bi_{12}TiO_{20-z}N_z$ ($z = 0.06$) powders were prepared. After annealing, the morphologies of as-synthesized samples exhibit sheet-like morphologies. And by controlling the amount of urea added in the precursor solutions, photocatalyst with sheet-like morphologies with good crystalline facet and larger surface area can be synthesized.

The absorption spectra of nitrogen-doped $Bi_{12}TiO_{20-x}N_x$ ($x = 0.01$), $Bi_{12}TiO_{20-y}N_y$ ($y = 0.03$), and $Bi_{12}TiO_{20-z}N_z$ ($z = 0.06$) films were successfully expanded from about 400 nm of $Bi_{12}TiO_{20}$ to about 500 nm, also from DRS spectra the band edge were successfully expanded from about 420 nm to about 460 nm, which would greatly enhance the utilization ratio of visible light in solar spectra. The expanded visible light can be attributed to the doping of nitrogen substituting of oxygen in $Bi_{12}TiO_{20}$ crystal lattice. Photocatalytic performance of nitrogen-doped $Bi_{12}TiO_{20-y}N_y$ ($y = 0.03$) with N/(N+O) mole ratio about 3% is better photocatalytic activity than that of undoped, light-doped (below 1%), and heavily doped $Bi_{12}TiO_{20-z}N_z$ ($z = 0.06$) photocatalysts.

Acknowledgments

This paper was financially supported by research grants from the National Basic Research Program of China (973 Program, no. 2007CB613302), and the National Science Foundation of China (nos. 20973102 and 51021062). The authors also express our thanks for the editor's patience.

References

[1] A. Fujishima, K. Honda, and S. Kikuchi, "Photosensitized electrolytic oxidation on semiconducting n-type TiO_2 electrode," *Kogyo Kagaku Zasshi*, vol. 72, pp. 108–113, 1969.

[2] A. Fujishima and K. Honda, "Electrochemical photolysis of water at a semiconductor electrode," *Nature*, vol. 238, no. 5358, pp. 37–38, 1972.

[3] J. A. Byrne, P. A. Fernandez-Ibañez, P. S. M. Dunlop, D. M. A. Alrousan, and J. W. J. Hamilton, "Photocatalytic enhancement for solar disinfection of water: a review," *International Journal of Photoenergy*, vol. 2011, Article ID 764870, 12 pages, 2011.

[4] J. Gamage and Z. Zhang, "Applications of photocatalytic disinfection," *International Journal of Photoenergy*, vol. 200, Article ID 764870, 11 pages, 2010.

[5] R. Asahi, T. Morikawa, T. Ohwaki, K. Aoki, and Y. Taga, "Visible-light photocatalysis in nitrogen-doped titanium oxides," *Science*, vol. 293, no. 5528, pp. 269–271, 2001.

[6] S. Sato, R. Asahi, T. Morikawa, T. Ohwaki, K. Aoki, and Y. Taga, "Photocatalysts sensitive to visible light—response," *Science*, vol. 295, no. 5555, pp. 626–627, 2002.

[7] K. Nukumizu, J. Nunoshige, T. Takata et al., "TiNxOyFz as a stable photocatalyst for water oxidation in visible light (<570 nm)," *Chemistry Letters*, vol. 32, no. 2, pp. 196–197, 2003.

[8] H. Liu and L. Gao, "(Sulfur, nitrogen)-codoped rutile-titanium dioxide as a visible-light-activated photocatalyst," *Journal of the American Ceramic Society*, vol. 87, no. 8, pp. 1582–1584, 2004.

[9] H. Liu and L. Gao, "Codoped rutile TiO_2 as a new photocatalyst for visible light irradiation," *Chemistry Letters*, vol. 33, no. 6, pp. 730–731, 2004.

[10] M. Mrowetz, W. Balcerski, A. J. Colussi, and M. R. Hoffmann, "Oxidative power of nitrogen-doped TiO_2 photocatalysts under visible illumination," *Journal of Physical Chemistry B*, vol. 108, no. 45, pp. 17269–17273, 2004.

[11] Q. Zhang, J. Wang, S. Yin, T. Sato, and F. Saito, "Synthesis of a visible-light active TiO_2-xSx photocatalyst by means of mechanochemical doping," *Journal of the American Ceramic Society*, vol. 87, no. 6, pp. 1161–1163, 2004.

[12] T. Matsunaga and M. Inagaki, "Carbon-coated anatase for oxidation of methylene blue and NO," *Applied Catalysis B*, vol. 64, no. 1-2, pp. 9–12, 2006.

[13] H. Yamashita, Y. Nishida, O. Chiyoda et al., "Design of efficient $TTiO_2$/SiC photocatalysts from TiC-SiC nano particles for degradation of organic pollutants diluted in water," *Materials Science Forum*, vol. 510-511, pp. 9–12, 2006.

[14] Y. Kesong, D. Ying, H. Baibiao, and H. Shenghao, "Theoretical study of N-doped TiO_2 rutile crystals," *Journal of Physical Chemistry B*, vol. 110, no. 47, pp. 24011–24014, 2006.

[15] H. Yamashita, Y. Nishida, S. Yuan et al., "Design of TiO_2-SiC photocatalyst using TiC-SiC nano-particles for degradation of 2-propanol diluted in water," *Catalysis Today*, vol. 120, no. 2, pp. 163–167, 2007.

[16] K. Yang, Y. Dai, and B. Huang, "Study of the nitrogen concentration influence on N-doped TiO_2 anatase from first-principles calculations," *Journal of Physical Chemistry C*, vol. 111, no. 32, pp. 12086–12090, 2007.

[17] J. A. Rengifo-Herrera, E. Mielczarski, J. Mielczarski, N. C. Castillo, J. Kiwi, and C. Pulgarin, "Escherichia coli inactivation by N, S co-doped commercial TiO_2 powders under UV and visible light," *Applied Catalysis B*, vol. 84, no. 3-4, pp. 448–456, 2008.

[18] G. Shang, H. Fu, S. Yang, and T. Xu, "Mechanistic study of visible-light-induced photodegradation of 4-chlorophenol by $TiO_{2-x}N_x$ ($0.021<x<0.049$) with low nitrogen concentration," *International Journal of Photoenergy*, vol. 2012, Article ID 759306, 9 pages, 2012.

[19] L. Zhao, J. Ran, Z. Shu, G. Dai, P. Zhai, and S. Wang, "Effects of calcination temperatures on photocatalytic activity of ordered titanate nanoribbon/SnO_2 films fabricated during an EPD process," *International Journal of Photoenergy*, vol. 2012, Article ID 472958, 7 pages, 2012.

[20] N.-H. Lee, H.-J. Oh, S.-C. Jung, W.-J. Lee, D.-H. Kim, and S.-J. Kim, "Photocatalytic properties of nanotubular-shaped TiO_2 powders with anatase phase obtained from titanate nanotube powder through various thermal treatments," *International Journal of Photoenergy*, vol. 2011, Article ID 327821, 7 pages, 2011.

[21] M.-L. Chen and W.-C. Oh, "The improved photocatalytic properties of methylene blue for V_2O_3/CNT/TiO_2 composite under visible light," *International Journal of Photoenergy*, vol. 2010, Article ID 264831, 5 pages, 2010.

[22] A. Kudo and S. Hijii, "H2 or O2 evolution from aqueous solutions on layered oxide photocatalysts consisting of Bi3+ with 6s2 configuration and d0 transition metal ions," *Chemistry Letters*, no. 10, pp. 1103–1104, 1999.

[23] S. Yao, J. Wei, B. Huang et al., "Morphology modulated growth of bismuth tungsten oxide nanocrystals," *Journal of Solid State Chemistry*, vol. 182, no. 2, pp. 236–239, 2009.

[24] W. F. Yao, H. Wang, X. H. Xu et al., "Photocatalytic property of bismuth titanate $Bi_{12}TiO_{20}$ crystals," *Applied Catalysis A*, vol. 243, no. 1, pp. 185–190, 2003.

[25] W. F. Yao, H. Wang, X. H. Xu et al., "Photocatalytic property of Zn-doped $Bi_{12}TiO_{20}$," *Journal of Materials Science Letters*, vol. 22, no. 14, pp. 989–992, 2003.

[26] W. F. Yao, H. Wang, X. H. Xu et al., "Characterization and photocatalytic properties of Ba doped $Bi_{12}TiO_{20}$," *Journal of Molecular Catalysis A*, vol. 202, no. 1-2, pp. 305–311, 2003.

[27] W. F. Yao, X. H. Xu, J. T. Zhou et al., "Photocatalytic property of sillenite $Bi_{24}AIO_{39}$ crystals," *Journal of Molecular Catalysis A*, vol. 212, no. 1-2, pp. 323–328, 2004.

[28] N. Thanabodeekij, E. Gulari, and S. Wongkasemjit, "$Bi_{12}TiO_{20}$ synthesized directly from bismuth (III) nitrate pentahydrate and titanium glycolate and its activity," *Powder Technology*, vol. 160, no. 3, pp. 203–208, 2005.

[29] X. H. Xu, W. F. Yao, Y. Zhang, A. Q. Zhou, Y. Hou, and M. Wang, "Photocatalytic properties of bismuth titanate compounds," *Acta Chimica Sinica*, vol. 63, no. 1, pp. 5–10, 2005.

[30] T. Lin, Z. Pi, M. C. Gong, J. B. Zhong, J. L. Wang, and Y. Q. Chen, "Gas-phase photocatalytic oxidation of benzene over titanium dioxide loaded on $Bi_{12}TiO_{20}$," *Chinese Chemical Letters*, vol. 18, no. 2, pp. 241–243, 2007.

[31] S. Xu, W. Shangguan, J. Yuan, J. Shi, and M. Chen, "Photocatalytic properties of bismuth titanate $Bi_{12}TiO_{20}$ prepared by co-precipitation processing," *Materials Science and Engineering B*, vol. 137, no. 1–3, pp. 108–111, 2007.

[32] S. Xu, W. Shangguan, J. Yuan, J. Shi, and M. Chen, "Preparations and photocatalytic degradation of methyl orange in water on magnetically separable $Bi_{12}TiO_{20}$ supported on nickel ferrite," *Science and Technology of Advanced Materials*, vol. 8, no. 1-2, pp. 40–46, 2007.

[33] J. Zhou, Z. Zou, A. K. Ray, and X. S. Zhao, "Preparation and characterization of polycrystalline bismuth titanate $Bi_{12}TiO_{20}$ and its photocatalytic properties under visible light irradiation," *Industrial and Engineering Chemistry Research*, vol. 46, no. 3, pp. 745–749, 2007.

[34] H. Zhang, M. Lü, S. Liu et al., "Preparation and photocatalytic properties of sillenite $Bi_{12}TiO_{20}$ films," *Surface and Coatings Technology*, vol. 202, no. 20, pp. 4930–4934, 2008.

[35] J. Hou, Y. Qu, D. Krsmanovic, C. Ducati, D. Eder, and R. V. Kumar, "Solution-phase synthesis of single-crystalline $Bi_{12}TiO_{20}$ nanowires with photocatalytic properties," *Chemical Communications*, no. 26, pp. 3937–3939, 2009.

[36] W. Wei, Y. Dai, and B. Huang, "First-principles characterization of Bi-based photocatalysts: $Bi_{12}TiO_{20}$, $Bi_2Ti_2O_7$, and $Bi_4Ti_3O_{12}$," *Journal of Physical Chemistry C*, vol. 113, no. 14, pp. 5658–5663, 2009.

[37] V. Marinova, "Optical properties of $Bi_{12}TiO_{20}$ doped with Al, P, Ag, Cu, Co and co-doped with Al + P single crystals," *Optical Materials*, vol. 15, no. 2, pp. 149–158, 2000.

[38] Z. Shuxian, W. K. Hall, G. Ertl, and H. Knözinger, "X-Ray photoemission study of oxygen and nitric oxide adsorption on MoS_2," *Journal of Catalysis*, vol. 100, no. 1, pp. 167–175, 1986.

[39] S. Badrinarayanan, S. Sinha, and A. B. Mandale, "XPS studies of nitrogen ion implanted zirconium and titanium," *Journal of Electron Spectroscopy and Related Phenomena*, vol. 49, no. 3, pp. 303–309, 1989.

[40] G. Soto, W. De La Cruz, and M. H. Farías, "XPS, AES, and EELS characterization of nitrogen-containing thin films," *Journal of Electron Spectroscopy and Related Phenomena*, vol. 135, no. 1, pp. 27–39, 2004.

[41] C. Ocal and S. Ferrer, "The strong metal-support interaction (SMSI) in Pt-TiO2 model catalysts. A new CO adsorption state on Pt-Ti atoms," *The Journal of Chemical Physics*, vol. 84, no. 11, pp. 6474–6478, 1986.